toxics

MDPI

Review

Biochar-Supported TiO_2-Based Nanocomposites for the Photocatalytic Degradation of Sulfamethoxazole in Water—A Review

Subhash Chandra [1,†], Pravin Jagdale [2,†], Isha Medha [1,3,*], Ashwani Kumar Tiwari [4], Mattia Bartoli [2], Antonio De Nino [5] and Fabrizio Olivito [5,*]

1 Department of Civil Engineering, Vignan's Institute of Information Technology (A), Duvvada, Visakhapatnam 530049, India; subhash2k6@gmail.com
2 Center for Sustainable Future Technologies, Italian Institute of Technology, Via Livorno 60, 10144 Torino, Italy; pravin.jagdale@iit.it (P.J.); mattia.bartoli@iit.it (M.B.)
3 Department of Mining Engineering, Indian Institute of Technology Kharagpur, Kharagpur 721302, India
4 School of Environmental Sciences, Jawaharlal Nehru University, New Delhi 110067, India; ashwaniktiwari@mail.jnu.ac.in
5 Department of Chemistry and Chemical Technologies, University of Calabria, Via P. Bucci, 87036 Rende, Italy; antonio.denino@unical.it
* Correspondence: medhaisha@gmail.com (I.M.); fabrizio.olivito@unical.it (F.O.); Tel.: +91-993-238-7436 (I.M.)
† These authors contributed equally to this work.

Abstract: Sulfamethoxazole (SMX) is a frequently used antibiotic for the treatment of urinary tract, respiratory, and intestinal infections and as a supplement in livestock or fishery farming to boost production. The release of SMX into the environment can lead to the development of antibiotic resistance among the microbial community, which can lead to frequent clinical infections. SMX removal from water is usually done through advanced treatment processes, such as adsorption, photocatalytic oxidation, and biodegradation. Among them, the advanced oxidation process using TiO_2 and its composites is being widely used. TiO_2 is a widely used photocatalyst; however, it has certain limitations, such as low visible light response and quick recombination of e^-/h^+ pairs. Integrating the biochar with TiO_2 nanoparticles can overcome such limitations. The biochar-supported TiO_2 composites showed a significant increase in the photocatalytic activities in the UV-visible range, which resulted in a substantial increase in the degradation of SMX in water. The present review has critically reviewed the methods of biochar TiO_2 composite synthesis, the effect of biochar integration with the TiO_2 on its physicochemical properties, and the chemical pathways through which the biochar/TiO_2 composite degrades the SMX in water or aqueous solution. The degradation of SMX using photocatalysis can be considered a useful model, and the research studies presented in this review will allow extending this area of research on other types of similar pharmaceuticals or pollutants in general in the future.

Keywords: sulfamethoxazole; photocatalysis; biochar; titanium oxide and antibiotic

check for updates

Citation: Chandra, S.; Jagdale, P.; Medha, I.; Tiwari, A.K.; Bartoli, M.; Nino, A.D.; Olivito, F. Biochar-Supported TiO_2-Based Nanocomposites for the Photocatalytic Degradation of Sulfamethoxazole in Water—A Review. *Toxics* **2021**, *9*, 313. https://doi.org/10.3390/toxics9110313

Academic Editor: Łukasz Chrzanowski

Received: 14 September 2021
Accepted: 29 October 2021
Published: 18 November 2021

1. Introduction

Water is an important resource for the living of animals, aquatic life, and human beings. During past decades, a continuous increase in the worldwide population and industrial activities have rapidly increased the water demand among the communities. Therefore, it is very much necessary to fulfil the water demand among the communities while maintaining the ecological balance [1]. However, due to the rapid industrialization and change in living style, the water quality in the natural resources such as rivers, lakes, and groundwater has substantially deteriorated due to the release of the pollutants [2,3]. In recent years, the production of antibiotics from pharmaceutical industries and their consumption by humans and animals has significantly increased due to the frequent endemic and pandemic episodes such as COVID-19, Ebola, and Swine flu [4,5]. The high

consumption of antibiotics by animals and human beings led to their excessive release into the environment [6]. The antibiotics remain poorly metabolized and can enter into the environment through various pathways such as human waste effluent, pharmaceutical waste, agricultural run-off, wastewater treatment plant effluent, and effluent waste from livestock farming [7–9]. Antibiotics are usually categorized as contaminants of emerging concern (CECs) due to their persistence in the environment. The availability of antibiotics in the environment either in altered or in metabolized forms enables the bacteria to develop a resistance against them, which is a point of major concern for public health due to the possibility of increasing the occurrence of related clinical infections [10]. Among the reported antibiotics, sulfamethoxazole (SMX) is of prime concern due to its widespread global uses, its ability to solubilize in water, and binding to the soil or organic matter through the cation exchange process [10]. The SMX, which is the most commonly used sulfonamide, is frequently prescribed to treat a wide variety of bacterial infections such as ear, urine tract, respiratory, and intestinal infections in human beings and other infections in aquaculture and livestock farming to boost production [11]. It is considered a persistent organic pollutant because its metabolites are stable compounds with certain toxicity [12]. Various studies reported the presence of SMX in the rivers, lakes, groundwater, and effluents of the water treatment plants having concentrations varying from 40–370 ng/L [13–15]. Conversely, the concentrations of SMX in the effluents from various wastewater treatment plants, pharmaceutical industries, and landfills are range from ng/L to several µg/L [16–18]. Therefore, the removal and degradation of this compound in the natural water system and effluent discharge is important to reduce its adverse effect on human beings, animals, and the ecosystem.

Several techniques of SMX removal from water have been mooted in the earlier studies consisting of adsorption using graphene and carbon nanomaterials, biodegradation, degradation using sonocatalysis, degradation under gamma radiation using Fe/C nanoparticles-based metal-organic framework (MOF), and oxidation using UV/H_2O_2 treatment [19–23]. All the reported methods have certain shortcomings; for example, the sonocatalysis process requires high energy to produce high-energy soundwaves that limit its scaling-up process, and the UV/H_2O_2 oxidation process is associated with the problem of generating toxic transformation byproducts [24,25]. In this context, the photocatalytic oxidation method has gained much attention for the degradation of SMX in water due to its low operational cost and high efficiency.

Various types of photocatalytic materials, such as TiO_2, ZnO and their carbon nanotube composites, were reportedly used for the photocatalytic degradation of SMX in water [26–28]. Among them, the TiO_2 nanoparticle was frequently used for the photocatalytic degradation of antibiotics under UV light exposure or in a combination of TiO_2 and H_2O_2 under UV exposure due to the availability of e^-/h^+ pairs, low band energy gap (3.20–3.35 eV), and high photocatalytic activities in the ultraviolet (UV) region [29]. However, the use of TiO_2 as the photocatalytic material for the degradation of SMX in water is very limited due to problems associated with the low adsorption capacity, high agglomeration, and quick recombination of e^-/h^+ within the narrow wavelength range (200–400 nm) [30]. Many studies came up with the solution to dope the TiO_2 nanoparticles with certain metals and carbon nanotubes to increase its photocatalytic sensitivity in the UV-visible range and reduce the band energy gap [31–33]. However, doping of the TiO_2 with the metals is associated with the problem of the release of the metals into the environment, which can have a toxic effect on the ecosystem [34]. Conversely, the doping of TiO_2 with CNTs is associated with the high cost of production, chances of increased recombination of e^-/h^+ pairs due to oxygen vacancies in bulk, and very limited long-term efficiency [30]. Hence, the integration of TiO_2 nanoparticles with biomass waste-derived carbon material called "biochar" has been mooted as a novel solution to counter the above-reported problems in many of the earlier studies [34,35].

Biochar is a porous carbon material derived through the pyrolysis of biomass waste in the temperature range of 300–800 °C [36]. The integration of biochar as a supportive

material for TiO_2 nanoparticles was reportedly done to increase the adsorption of SMX onto the micro- and mesopores of biochar, reduce the band energy gap, and reduce the chances of the recombination of e^-/h^+ pairs due to the high semi-conductor activity of the material [37]. The motivation for writing a review on the photocatalytic degradation of SMX in water using the biochar-TiO_2 composite material lies in the fact that, till now, various reviews have been published on the photocatalytic degradation of dyes, organic pollutants, and other antibiotics. However, not a single review is available particularly focusing on the speciation of SMX in water and its photocatalytic degradation using the biochar-supported TiO_2 composite. The objectives of this paper are to review the following:

(i) Synthesis methods of biochar-supported TiO_2 nanoparticles;
(ii) The effect of the integration of biochar with TiO_2 particles in terms of changes in the physicochemical properties and increase in the photocatalytic response under UV-visible light;
(iii) Delineate the photochemistry of SMX in water and its major sources into the environment;
(iv) Delineate the chemical pathways and mechanisms involved during the photocatalytic degradation of SMX in water using the biochar-supported TiO_2 nanoparticles.

2. Recent Degradation Techniques of the Common Antibiotics

Previous study results indicated that the application of TiO_2-biochar composite showed up to 90% removal of SMX from the aqueous solution via photocatalysis under UV-visible radiation [38]. Another study showed that more than 80% of SMX was removed from the aqueous solution having high chemical oxygen demand via photocatalysis using the TiO_2/biochar composite material [39]. Avramiotis and co-workers [40] developed a procedure to oxidize sulfamethoxazole through the activation of the persulfate by a pre-synthesized rice husk biochar, and they focused the study on the crucial activity of either electron transfer/singlet oxygen control and surface-bound radicals. In another recent work [41], in which SMX was indicated as a dangerous and recalcitrant pollutant, this antibiotic was degraded by the surface coating of a ceramic membrane by a photo-Fenton catalyst, and the degradation reached up to 90%. In a similar work carried out by Liu and co-workers [42], sulfonamide antibiotics were degraded efficiently using a combination of persulfate and UV irradiation. Vignati et al. [43] proved that ZnO can accelerate the photocatalytic degradation of Spiramycin in urban wastewater, and they carried out an in-depth study of the kinetics of the degradation and toxicity of the metabolites. In another work [44], the photocatalytic degradation of tetracycline hydrochloride under visible light irradiation using a newly synthesized photocatalyst MVO_4/g-C_3N_4 (M = La, Ga) prepared by a hydrothermal method was investigated.

3. Sulfamethoxazole (SMX) in Water

3.1. Sources of Sulfamethoxazole in Water and Their Environmental Impacts

There are various point and non-point sources of SMX in rivers and other water resources. The major sources of SMX (antibiotic) into water are illustrated graphically in Figure 1. The primary sources of this molecule into the water resources can be classified into five different groups: (i) effluent wastes from hospitals, (ii) effluent waste from pharmaceutical industries, (iii) effluent waste from the water treatment plant, (iv) effluent waste from aquaculture system and livestock farming, and (v) effluent and leachates from sanitary landfills [45]. The concentration of SMX in the river stream and water reportedly varies from ng/L to mg/L [45]. The SMX from the aquaculture system and livestock farming mostly come into the river stream through the disposal of wastewater generated from the farms directly into the river. The concentration of SMX from aquaculture systems (fish and shrimp) and livestock farms (pig and poultry) reportedly varies from 10 µg/L to 7 mg/L as reported in the water samples collected from shrimp ponds and canals nearby the livestock farming in Vietnam [46,47]. Untreated sewage is another source of SMX into the water as, during the heavy rainfall, untreated sewage, due to having limited hydraulic capacity, finds its way into the freshwater line. The concentration of SMX from the sewage

discharge reportedly varies from ng/L up to 60 µg/L, as indicated by the data of the analysis of water samples from the sewage line discharge and freshwater streams within its nearby areas [48]. Apart from that, the presence of SMX in the effluent of wastewater treatment plants was also observed in the water samples, as reported in studies conducted in different countries [49,50]. The concentration of this compound in the effluent of sewage treatment plants reportedly varies from 226 to 3000 ng/L as per the data obtained from different studies conducted in China, Vietnam, and the Philippines [47,51,52]. Leachate from landfills is another major source of SMX discharge into the surface and groundwater. However, very little information and understanding of the mechanism is available regarding the fate and transport of this compound from the landfill sites. The concentration of SMX in the leachates reportedly varies from 6.4 to 8488 ng/L based on the data gathered from the studies conducted in the landfill sites of China and Singapore [53,54]. Moreover, the effluent waste from the pharmaceutical industries and hospital wastes are categorized as one of the direct sources of SMX and other antibiotics into the water. Previous studies carried out in the cities of China and Vietnam indicated the presence of SMX and other antibiotics in wastewater generated from hospitals and pharmaceutical industries [55,56]. The typical concentration of SMX in the wastewater generated from the pharmaceutical industry and hospitals reportedly varied from 320–2910 ng/L based on the data of the studies done earlier in China and Vietnam [55,57].

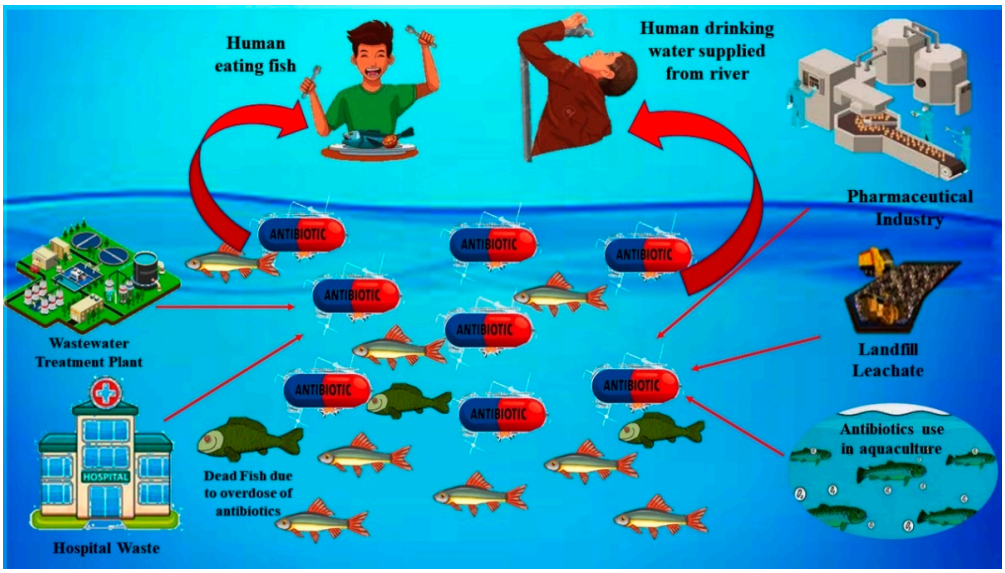

Figure 1. Graphical illustration of various point and non-point sources of SMX into the rivers and water resources.

3.2. Photochemistry of Sulfamethoxazole in Water

Sulfamethoxazole (SMX) and tetracycline are widely used antibiotics, which are mostly used for the treatment of human beings and animals [58]. These antibiotics are usually detected in wastewater, surface water, and groundwater in the detection range of ng L^{-1} to µg L^{-1} [59,60]. Specifically, sulfamethoxazole (SMX), which comes under the chemical class of sulfonamide compounds, is an antimicrobial drug with broad-spectrum activity against gram-positive and negative bacteria [61]. The pharmaceutical waste, of which the antibiotic is a part, is usually hydrolyzed in water. The understanding of the degree and behavior of hydrolysis of antibiotics is of prime concern to understand their stability and non-biodegradability in the environment [62]. Sulfamethoxazole possesses good chemical stability in the environment, which allows it to resist metabolic processes and natural degradation [63]. The SMX usually absorbs the incident radiation light in the wavelength range of 250 to 300 nm, which also varies with respect to the change in the surface charge density on the SMX as the pH of the aqueous solution varies from acidic to alkaline [64].

The absorbance range reportedly shifted towards a higher wavelength side (up to 300 nm) as the pH of the aqueous solution was reduced to 1 from 10 (Figure 2) [64]. The pH of the solution plays a key role in the photocatalytic decomposition of SMX in water, as the SMX degradation rate reportedly was decreased with the increase in the pH value of the aqueous solution, as shown in Figure 3a [28]. The SMX mostly exists in the anionic form if pH > 5.6, and in the neutral form if pH lies between 1.85–5.6 (Figure 3b), as the pK_{a1} and pK_{a2} values of SMX was reported to be about 1.85 and 5.60, respectively [28,64]. The photolytic degradation of SMX is very difficult as it cannot be completely mineralized during oxidation [28]. Previous studies elucidated the photocatalytic oxidation mechanism of SMX and the formation of intermediatory transformation products (TPs) [28,64]. The detailed mechanism of SMX photodegradation in the presence of reactive oxygen species (ROS), i.e., •OH radical is shown in Figure 4. It can be observed from the figure that SMX formed its isomerization intermediatory product and is denoted by P 254. Subsequently, with the addition of •OH radical, the SMX is degraded to an intermediatory product denoted by 270 c. Thereafter, the addition of •OH radical to the transformation product (TP) defined as 270 c led to the demethylation process, which resulted in the formation of a new TP denoted by P 288. Subsequently, the breakage of the N–O bond and the removal of the carboxylic group from P 288 lead to the formation of another TP denoted by P 246. Additionally, the release of N–O and C–C bonds from P 288 formed another intermediatory product or TP denoted by P 198. The cleavage of the S–N bond from the SMX structure was reportedly occurred after reacting with an •OH free radical following the binding of N to an H atom, which leads to the formation of another TP called 3-amino 5-methylisoxazole denoted as P 99 [64]. The isomerized product of SMX is denoted by P 254, which, after reacting with •OH free radical, leads to the scission of S–N bond from P 254 that leads to the formation of a TP denoted by P 174. The P 174 on further oxidation with ROS leads to the formation of two new TPs denoted as P 158 and P 95, respectively, following the loss of C–N and C–S bonds.

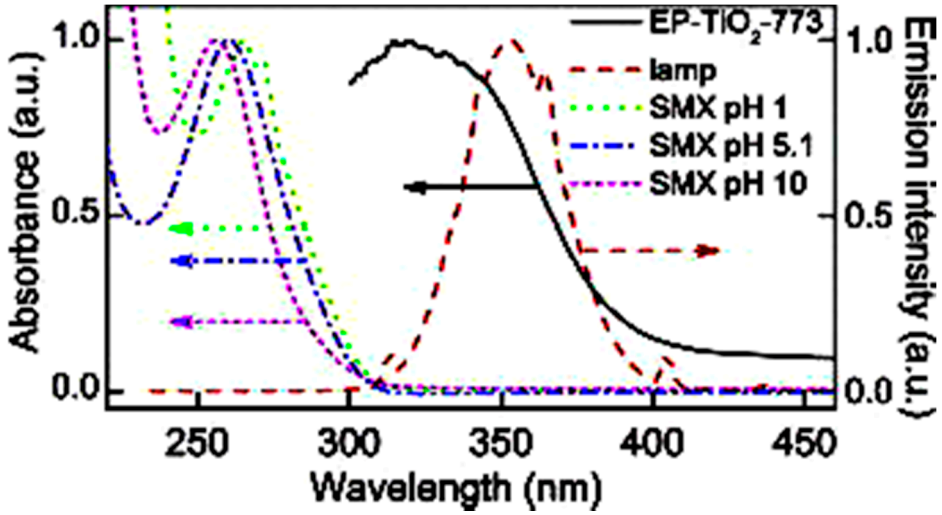

Figure 2. Variations in the wavelength absorbance by SMX with the change in the pH of the aqueous solution (reproduced from [64], Copyright Year 2015, Journal of Hazardous Material @ Elsevier with the permission order number: 5114720328428) (EP-TiO_2: Expanded perlite coated TiO_2 particles).

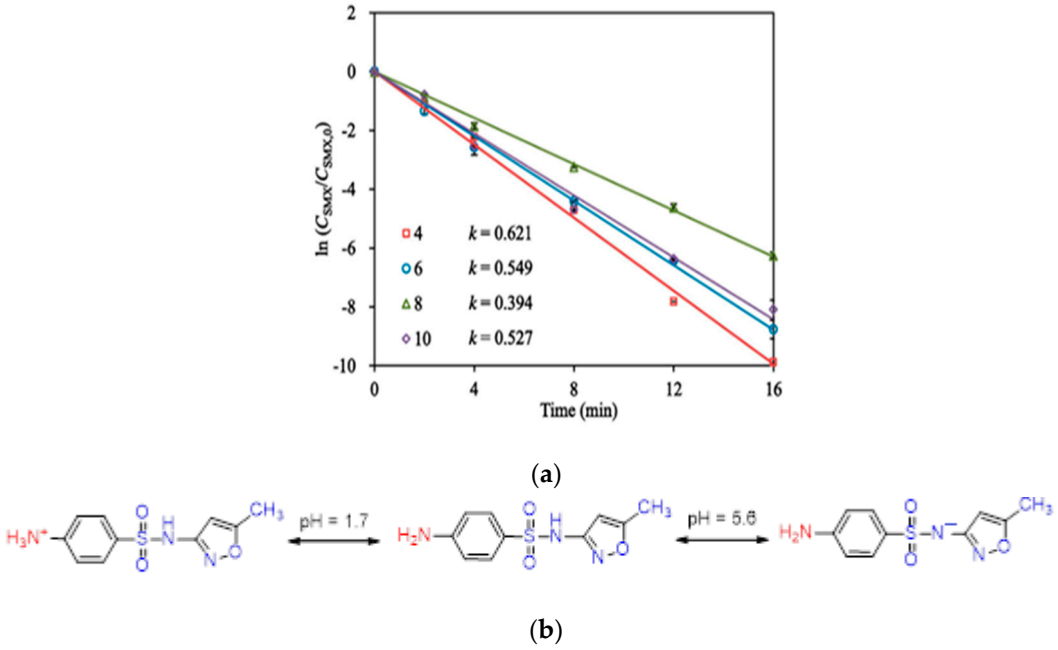

Figure 3. (**a**) Variations in the photocatalytic degradation of SMX concerning change in the pH of the aqueous solution (Reproduced from [22] (with the permission order number: 5114291052991); (**b**) charge variation in the structure of SMX with respect to the change in pH from acidic to alkaline in the aqueous solution (adapted from [64], Copyright Year 2015, Journal of Hazardous Material @ Elsevier with the permission order number: 5114720328428).

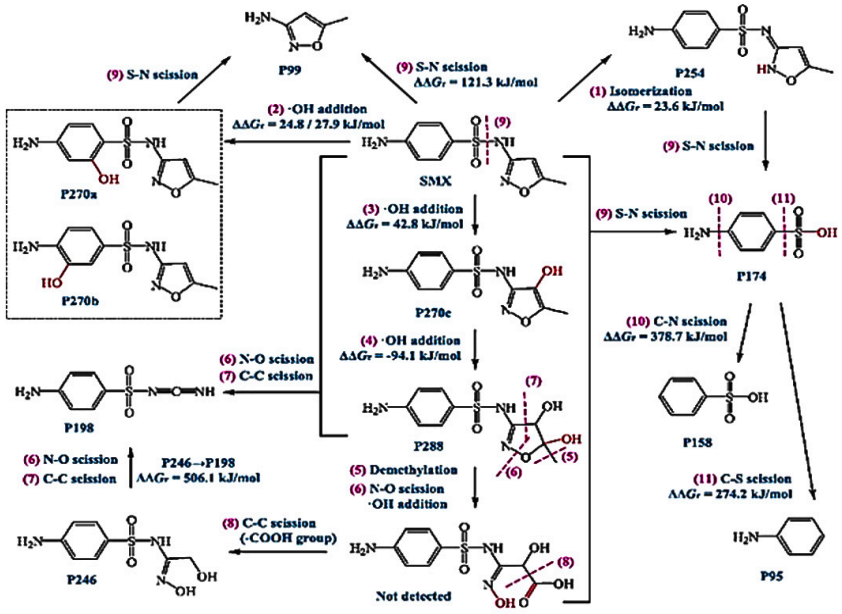

Figure 4. Mechanism of photolytic oxidation/reduction of SMX and the formation of various transformative products (TPs) during its photolysis (reproduced from [28] Copyright Year 2019, Chemical Engineering Journal @Elsevier with permission License number: 5114291052991© Elsevier).

4. Synthesis of Biochar-Supported TiO_2 Nanocomposites

Titanium oxide (TiO_2) is a conventionally used a very common type of photocatalytic material reported in many of the earlier studies for the photocatalytic oxidation/reduction of the pollutants in the aqueous solution due to having a very stable chemical structure and non-toxicity [65]. Despite having photocatalytic properties and stable structure, nowadays, TiO_2 nanoparticles are not commonly used for the photocatalytic oxidation of pollutants in water. The reason behind its limited use for photocatalytic actions can be linked to

its high bandgap (3.20 eV) and very narrow light absorbance in the ultraviolet-visible (UV-visible) range (200–400) [65,66]. Hence, TiO_2 nanoparticles were reportedly chemically integrated with various materials, such as Zn nanoparticles, graphene, carbon nanotubes (CNT), activated carbon, and biochar, to reduce the band energy gap and increase the UV-visible absorbance range [67–70]. Among the above-reported supporting materials to synthesize the TiO_2 composite, biochar has gained much attention due to its sustainability and low cost compared to the other reported materials. Moreover, the biochar-based nanoparticles reportedly have varieties of tunable functional groups, high chemical and thermal stability, and high electrical conductivity that, when integrated with the TiO_2 nanoparticles, can reduce the bandgap and quick recombination of e^-/h^+ pairs during photocatalysis [38]. The biochar-supported TiO_2 composite can be developed using various physical, chemical, and thermal methods whose details are comprehensively covered in the subsequent sub-sections.

4.1. Sol–Gel Method

Sol–gel is the most widely used method reportedly used for the synthesis of biochar-supported TiO_2 nanocomposites (Figure 5A) [71–73]. In this method, the biomass is converted to biochar through the pyrolysis process [36], and then, the produced biochar is chemically treated with some weak acids, such as acetic or acrylic acid, to increase the surface oxides and reduce its pH [74,75]. Subsequently, the acid-treated biochar is then mixed with the slurry containing TiO_2 nanoparticles in ethanol. The entire slurry mixture is then filtered through 0.22 µm filter paper to separate solid from liquid fraction. The solid fraction of the slurry is then calcinated in the temperature range of 500–700 °C to produce a highly stable biochar-supported TiO_2 nanocomposite [76,77]. In the calcination process, the calcination temperature plays an important role, as heating the biochar TiO_2 mixture above 700 °C reportedly changes the TiO_2 crystal structure from anatase to rutile form [77].

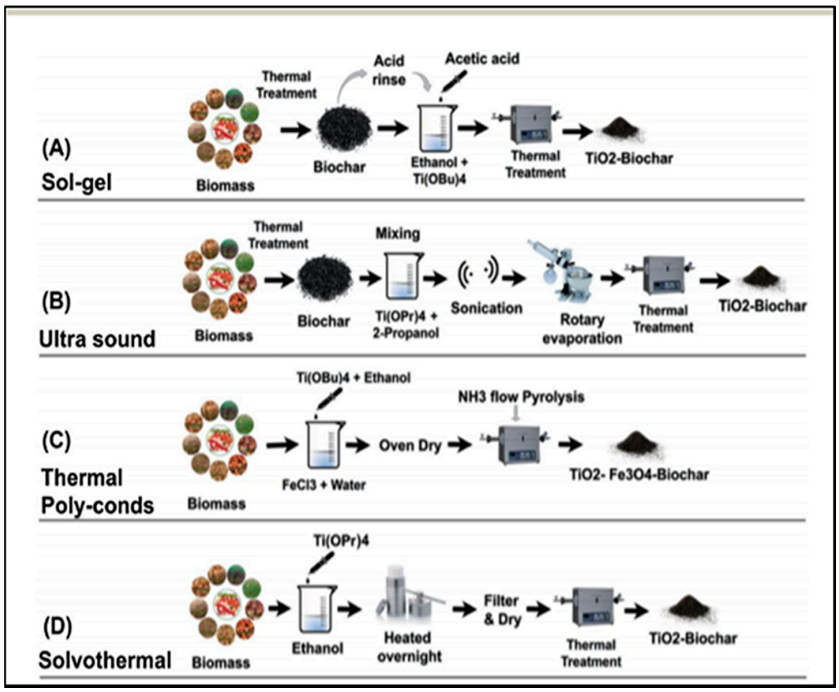

Figure 5. Illustration of various methods to develop biochar-supported TiO_2 nanocomposite material for photocatalysis: (**A**) Sol-gel method, (**B**) Ultra sound method, (**C**) Thermal Polycondensation method, and (**D**) Solvothermal method for the synthesis of biochar supported TiO_2 nanocomposite (reproduced from [73] Copyright year 2018, RSC Advances with permission under Creative Commons Attribution 3.0 Unported Licence).

4.2. Ultrasound Method

The ultrasound method is similar to the sol-gel method with the addition of an extra process of ultrasonication. The sonication of the pristine biochar with TiO_2 in the organic aqueous solution is done to promote the impregnation of TiO_2 nanoparticles into the pore of the porous biochar structure, which, upon calcination, reportedly provides a surface for TiO_2 crystal growth [78]. The detailed procedure of the synthesis of biochar-supported TiO_2 nanocomposite using the ultrasound method is illustrated in Figure 5B. Briefly, the biomass is converted to biochar through the pyrolysis process. The produced biochar after the crushing and sieving process is mixed with the Titanium isopropoxide and 2-propanol solution in a certain weight-by-volume ratio, and then, the mixture is subjected to the ultrasonication process for around 1–2 h. The ultrasonication of biochar and Titanium isopropoxide is done to break the biochar particles to nanoscale and to produce cracks on its surface, in which, subsequently, the TiO_2 nanoparticles are reportedly embedded [76]. The TiO_2-embedded biochar nanoparticles are then calcinated in the temperature range of 500–700° to start the nucleation of TiO_2 crystals within the cracks present in the biochar particles to produce a biochar-supported TiO_2 nanocomposite material.

4.3. Thermal Polycondensation Method

The thermal polycondensation process is also known as the single-step heating process to produce biochar-supported TiO_2 nanoparticles, as illustrated in Figure 5C [79,80]. In this method, the biomass is initially mixed with some precursor such as melamine or polysaccharide agar to increase its thermal response during the calcination process. After that, the resultant biochar is mixed in a diluted ethanol solution containing titanium butyrate. The resulting solution mixture is oven-dried and then subjected to the calcination process under an ammonia gas environment to decrease the band energy gap and improve the visible light response of the biochar-supported TiO_2 nanocomposite during the photocatalysis process [76,80].

4.4. Solvothermal Method

Solvothermal is the combination of hydrothermal treatment and dry heating process that facilitates the growth of TiO_2 crystals onto the biochar's surface, as shown in Figure 5D. In this method, the biomass is dispersed into an ethanol solution containing titanium isopropoxide in different (w/w) ratios, such as 1:1 or 1:2, and then, the entire mixture containing biochar particles and titanium isopropoxide is subjected to a hydrothermal process in the temperature range of 160–175 °C for a duration of 12–14 h [71,72]. Subsequently, the solids are separated from the mixture solution through the filtration process. The collected solid particles are washed several times with distilled water and then subjected to a calcination process in the temperature range of 600–700 °C for 6–8 h. The resultant is usually termed as biochar-supported TiO_2 nanocomposite particles [73].

5. Effect of Biochar Addition on the Chemical and Structural Characteristics of TiO_2 Nanoparticles

Titanium dioxide is the most commonly used photocatalytic material reportedly being used for the photocatalytic degradation of pollutants in water under an advanced oxidation process (AOP). The pollutants are degraded by the charged radicals generated from TiO_2 when illuminated under light with a wavelength less than 400 nm, as shown in Figure 6a. However, the use of TiO_2 as a photocatalytic material for the oxidation/reduction of pollutants has certain limitations, such as a narrow photocatalytic activity region ($\lambda < 400$ nm), i.e., the very limited photocatalytic activity of the materials within the wavelength of the visible range (401–700 nm) (Figure 6b), quick recombination of e^-/h^+ pairs due to having large energy bandgap (~3.20 eV), very poor affinity towards organic pollutants, such as antibiotics, and the problem of agglomeration [74]. Hence, to overcome the limitations, the combination of the TiO_2 nanoparticles with a sustainable porous carbon material called

"biochar" to produce biochar-supported TiO_2 nanocomposite for enhanced photocatalytic activities was mooted in the earlier studies [75,76].

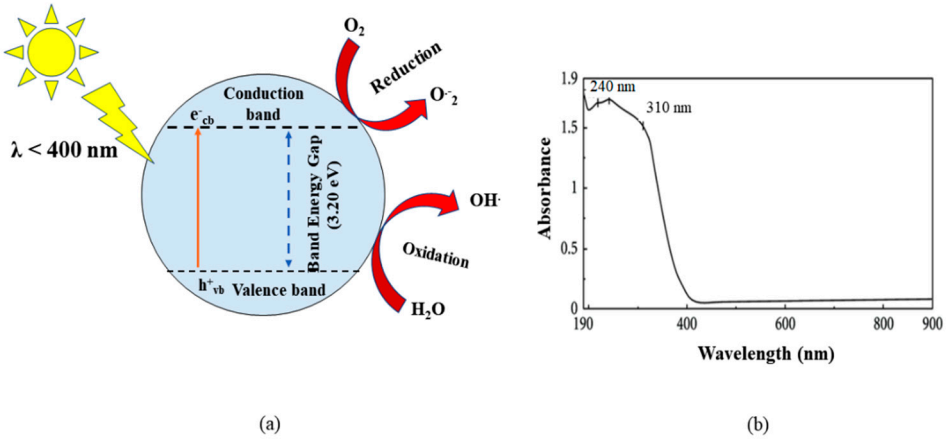

Figure 6. (**a**) Mechanism of generation of charged radicals from TiO_2 upon illumination within wavelength less than 400 nm; (**b**) UV-visible absorbance by TiO_2 particles within the wavelength range of 200–800 nm (reproduced from [77] Copyright 2012, International Journal of Photoenergy with permission under creative commons attributions 4.0 License).

The rationale behind the integration of biochar particles with TiO_2 nanoparticles can be linked to the fact that the presence of biochar with TiO_2 nanoparticles reportedly increased the adsorption of pollutants on the composite's surface, thereby increasing the photocatalytic degradation rates. Moreover, the biochar addition to the TiO_2 nanoparticles reportedly increased the available electrons in the conduction band to generate charged oxygen and hydroxyl radicals through the reduction and oxidation process, respectively, due to the availability of free electrons on the biochar's surface [70]. The major changes observed after the integration of biochar with the TiO_2 nanoparticles were the change in the morphological structure, UV-visible absorbance range, and mineralogical structures, as shown in Figures 7 and 8. It can be observed from Figure 7 that the biochar has a porous carbon structure that, after integration with TiO_2 particles, provided a nucleation site during the calcination process within the pores for the crystallization of TiO_2 nanoparticles within the biochar's pore structure that can be seen in the form of granules on the biochar's surface [38]. Additionally, the diffraction peaks at 2θ angles of 25.3, 37.8, 48.1, and 54.1 in the biochar-supported TiO_2 reportedly indicate the presence of anatase TiO_2 within the biochar structure, which confirms the successful integration of TiO_2 in the biochar structure [38]. Further, the peaks at the 2θ angles of 62.5 and 70° are reportedly due to the presence of carbonates and CaO in the biochar's structure [64]. The UV-visible absorbance (Figure 8a) showed that the TiO_2 did not show any absorbance in the visible range (λ = 400–700 nm) but showed an absorbance of 1.4 (A.U) within the UV range (λ = 200–400 nm). However, the UV-visible absorbance of biochar-supported TiO_2 showed a significant increase in the absorbance within both UV and visible light range unlike only in the UV range, as shown by the TiO_2 nanoparticles. Apart from that, by increasing the pyrolysis temperature of the biochar from 550 to 700 °C, the UV-visible range light absorbance in the biochar-supported TiO_2 nanocomposite was significantly increased due to an increase in the available free electrons in the biochar structure [78,79]. The high-resolution transmission electron microscopy (HRTEM) image of the biochar-supported TiO_2 nanocomposite reportedly showed the presence of anatase TiO_2 on the carpet-like biochar's surface [78]. The HRTEM image (Figure 8b) confirmed the proper integration of TiO_2 particles within the biochar's structure. Thus, it can be observed that the integration of TiO_2 nanoparticles with the biochar's structure significantly changed the chemical characteristics of the resulting biochar-supported TiO_2 nanocomposite. This makes it an efficient photocatalytic material for the photocatalytic degradation of the pollutants

in the aqueous solution by increasing the light absorbance range, decreasing the e^-/h^+ recombination, reducing the band energy gap, and increasing the surface interaction of the pollutants with the nanocomposite surface, thereby increasing its photocatalytic activity.

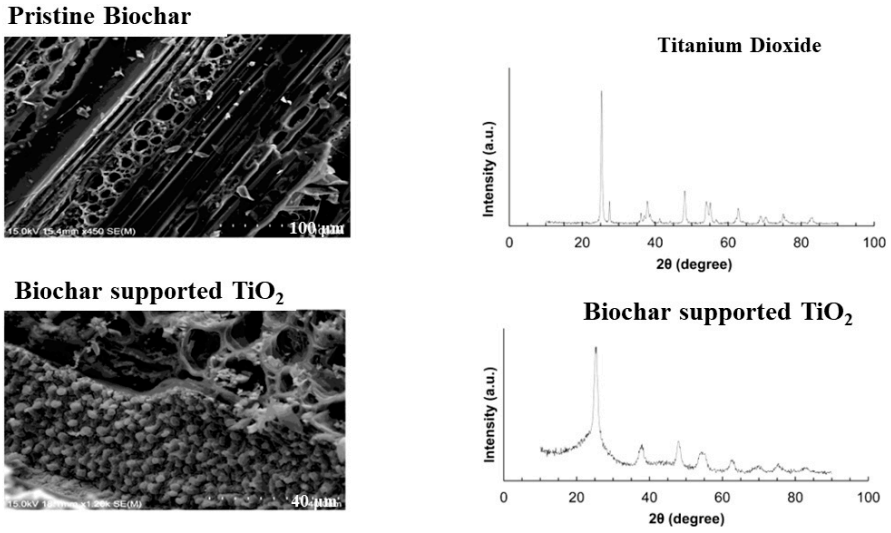

Figure 7. SEM and XRD pattern of the pristine biochar and biochar-supported TiO_2 nanoparticle (reproduced with permission from [38] Copyright Year 2016, Journal of Environmental Management © Elsevier Pvt Ltd. License number 5122010796759).

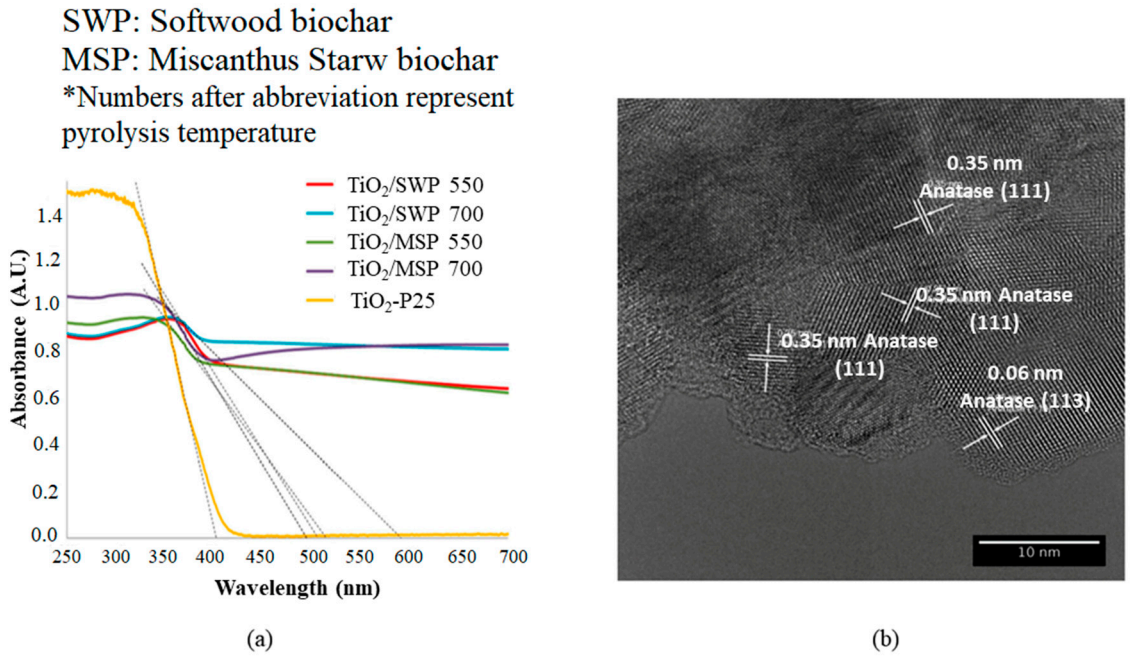

Figure 8. (**a**) UV-Visible absorbance of TiO_2 and biochar-supported TiO_2 (BSTPs) nanocomposites; (**b**) High-resolution transmission electron microscope image (HRTEM) of BSTPs (reproduced with permission from reference [78] copyright © 2021, American Chemical Society).

6. Application of Biochar-Supported TiO_2 Nanoparticles for the Photocatalytic Degradation of Sulfamethoxazole

The removal of SMX using various techniques such as ozonation, reverse osmosis, membrane filtration, adsorption, biological treatments, and advanced oxidation has been mooted in the previous studies [61,80–85]. Among them, the advanced oxidation process is an emerging technique for the removal of the antibiotic from water due to the low cost

of material synthesis, simple operation, and high efficiency of removal [86]. The removal efficiency of the wastewater containing SMX using the biochar-supported TiO_2 and its comparison with respect to the only TiO_2 under UV light source, without any photocatalyst under UV light, and without any catalyst under simulated sunlight is shown in Figure 9. It can be evinced from the figure that SMX degradation under simulated sunlight and UV light source without any addition of photocatalyst was very appreciable (20–50%) [87]. However, the removal efficiency of SMX with the addition of TiO_2 as a photocatalytic material under UV light illumination was increased to up to 60%. Furthermore, this removal efficiency was substantially increased to more than 90% when the solvent was mixed with biochar-supported TiO_2 composite photocatalytic material, indicating the higher photocatalytic activity of the biochar-TiO_2 composite compared to the only TiO_2 particles. Moreover, it can also be observed that the SMX was photo catalytically removed in the presence of COD in the solvent, whose removal percentage was also reportedly increased from 42 to 60% with the addition of biochar-TiO_2 compared to the singularly applied TiO_2 particles. Thus, the above result suggested that the removal efficiency of SMX was not compromised due to the presence of other organic and inorganic pollutants under photocatalytic degradation.

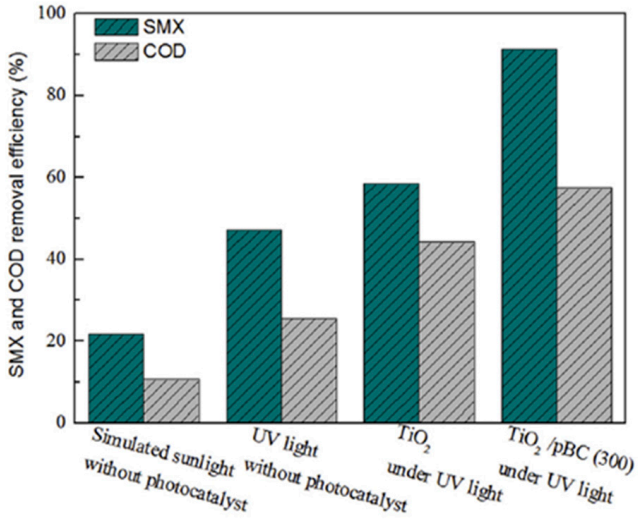

Figure 9. Photochemical degradation of SMX and COD under sunlight and UV light using TiO_2/pBC composite (Initial SMX concentration = 10 mg/L, Photocatalyst dose = 0.2 g) (Reproduced from [88] Copyright Year 2017, Chemosphere with the permission License number: 5141190415626).

In Table 1, the data related to the photocatalytic removal of SMX from the water using the biochar-TiO_2 composite, TiO_2-CNT composite, and other TiO_2 nanocomposites are given. It can be observed from the table that among all the listed TiO_2 composites, the maximum removal efficiency of SMX from the water was shown by the biochar-TiO_2 composite (91.27%) produced using the sol–gel method under the UV range (200–400 nm), followed by ZnO-TiO_2 biochar composite (81.21%) and the multiwalled carbon nanotube (MWCNT)/TiO_2 composite (90%). The reduced graphene oxide (RGO)/TiO_2 showed a removal efficiency of 77.27% for the SMX removal from water or aqueous solution. Apart from the above-mentioned TiO_2 composites, all the other forms of TiO_2 composites, such as Cu-TiO_2, clay-TiO_2, and TiO_2-borosilicate composites, reportedly showed a relatively lower SMX removal efficiency in water or aqueous solution (70–80%, Table 1). Moreover, it can also be observed that the photocatalytic removal efficiency of SMX using biochar/TiO_2 was significantly ($p < 0.05$) decreased from 91.27 to 40.58% with the increase in the pH of the aqueous solution from 4 to 10.77. The decrease in the photocatalytic removal efficiency of SMX using the biochar/TiO_2 composite with the increase in the pH of the aqueous solution can be linked to the pKa values of the SMX and biochar/TiO_2 composite. The SMX reportedly has two pKa values (pKa = 1.7 and pKa = 5.6), which suggests that the SMX

remained in the cationic form if the pH of the solution is less than 1.7 and in the anionic form if the pH > 5.6 units [89]. Additionally, the pKa value of the biochar/TiO_2 composite was 6.1, indicating that the surface of biochar/TiO_2 composite remained positively charged if the pH of the solution remained below 6.1; otherwise, it was negatively charged [90]. Hence, in the acidic pH condition (pH = 4), the biochar/TiO_2 surface remained positively charged, which might have electrostatically attracted the negatively charged structure of SMX on its surface for adsorption. After adsorption of the SMX on the biochar/TiO_2 surface, the SMX is reportedly degraded by the •OH radical produced via photocatalysis of the biochar/TiO_2 composite. The integration of biochar as a supportive material with the TiO_2 reportedly helps the photocatalytic degradation of organic pollutants in two ways: firstly, by providing the adsorption sites on its porous surface due to the availability of pores and high specific surface area, and secondly, having the ability to prevent the recombination of e^- and h^+ pair due to having an abundance of π-electrons and low energy bandgap that eventually promotes the generation of •OH from the catalyst [91]. The detailed mechanism of SMX photocatalytic degradation in the aqueous solution is illustrated in Figure 9. The biochar/TiO_2 photocatalytic composite reportedly photogenerates a h^+ and e^- pair upon incidence with high photon energy that is sufficient enough to excite the h^+ and e^- pair from the valance to conduction band. The photogenerated h^+ is freely available on the surface of TiO_2, which, upon reaction with H_2O, reportedly produces •OH radical [92]. Similarly, the freely available e^- in the conduction band of TiO_2 reportedly reacts with O_2 to generate O_2^- [93,94]. The detailed reactions to produce •OH and O_2^- are given in Equations (1)–(6) [88]. Both of the radicals, i.e., OH and O_2^-, reportedly have a very strong ability to oxidize the SMX and its intermediates to some inorganic forms [88]. The chemical reactions depicting the photocatalytic generation of •OH and O_2^- are given in Equations (1)–(6) as follows [77]:

$$TiO_2/BC + h\nu \rightarrow h^+ + e^- \quad (1)$$

$$h^+ + H_2O \rightarrow \bullet OH\cdot + H^+ \quad (2)$$

$$OH^- + H^+ \rightarrow \bullet OH \quad (3)$$

$$e^- + O_2 \rightarrow O_2^- \quad (4)$$

$$O_2^- + H_2O \rightarrow \bullet OH_2 + O_2^- \quad (5)$$

$$\bullet OH_2 + H_2O + e^- \rightarrow H_2O_2 + OH^- \quad (6)$$

Table 1. Photocatalytic degradation of Sulfamethoxazole (SMX) at different experimental conditions using biochar-supported TiO_2 nanocomposite and other hybrid TiO_2 composites.

S. No.	Type of Photocatalyst	Synthesis Method	pH	Light Irradiation Range	SMX Removal (%)	References
1	UV light without photocatalyst	-	4	UV range (200–400 nm)	47.24	[88]
2	TiO_2	-	4	UV range (200–400 nm)	58.47	
3	TiO_2/Biochar	Sol–gel	4	UV range (200–400 nm)	91.27	
4	TiO_2/Biochar	Sol–gel	5.95	UV range (200–400 nm)	82.24	
5	TiO_2/Biochar	Sol–gel	8.53	UV range (200–400 nm)	65.17	
6	TiO_2/Biochar	Sol–gel	10.77	UV range (200–400 nm)	40.58	

Table 1. *Cont.*

S. No.	Type of Photocatalyst	Synthesis Method	pH	Light Irradiation Range	SMX Removal (%)	References
7	RGOT/SA (Reduced graphene oxide TiO_2/Sodium alginate)		-	UV range (200–400 nm)	77.6	[95]
8	MCNT/TiO_2 (Multiwalled carbon nano tube/TiO_2)	Acid catalysed Sol–gel	-	UV range (200–400 nm)	90	[96]
9	TiO_2/Biochar	Sol–gel	-	UV range (200–400 nm)	91	[38]
10	ZnO-TiO_2/Biochar	Modified Sol–gel	3.95	UV irradiation ($\lambda < 410$ nm)	78.34	[39]
11	ZnO-TiO_2/Biochar		5.03		81.21	
12	ZnO-TiO_2/Biochar		6.92		75.48	
13	ZnO-TiO_2/Biochar		8.95		71.10	
14	Clay-TiO_2 composite	Sol–gel	-	UV irradiation	70.2	[97]
15	Cu-TiO_2	Sol–gel	-	UV-visible (300–800 nm)	94%	[98]
16	TiO_2-GAC-MPR (Activated Carbon-Membrane photobioreactor	Sol–gel	-	UV irradiation	83.60	[99]
17	TiO_2-Borosilicate Glass	Solvothermal	-	UV irradiation	70	[100]
18	Bi_2O_4–TiO_2	Hydrothermal	5.0	UV-Visible (190–1100 nm)	90	[101]

The generated •OH and O_2^- radicals oxidize the SMX in the aqueous solution through three different pathways: hydroxylation, the opening of the isoxazole ring, and cleavage of the S–N bond [87]. Several intermediates produced during the photochemical degradation of SMX in water through •OH and O_2^- radicals have been identified using HPLC chromatogram in a previous study [88]. During the hydroxylation process, the hydroxyl radical •OH reportedly attacks the benzene ring, isoxazole ring, and the amine group in the SMX. The detailed mechanism of the photochemical degradation of SMX in water or aqueous solution is illustrated in Figure 10.

From the figure, it can be observed that the SMX, upon oxidation by the hydroxyl radical (•OH), deteriorates in three different ways. First is the hydroxylation process, in which a hydroxyl group is attached to the carbon ring, the isoxazole ring, and relaces the amine group in the carbon ring, leading to the formation of three intermediates C1, C2, and C3 with m/z values of 269.81 and 254.81, respectively. The intermediate C1 upon further oxidation by the •OH leads to the formation of a stable product denoted by C5 with an m/z value of 227.95. Moreover, the further oxidation of C2 and C3 intermediates leads to the attachment of the oxygen group in the isoxazole ring, resulting in the formation of another two intermediates, namely C4 and C5 with m/z values of 287.33 and 269.82, respectively. These intermediates (C4 and C5) upon further oxidation by •OH radical reportedly cause the cleavage of the isoxazole ring from the carbon ring attached through

the link of the sulphate group, resulting in the formation of stable end products denoted as C7 and C8 with m/z values of 174.83 and 144.84, respectively [88]. Besides this, there are two more ways through which the SMX oxidizes to the stable end products. Firstly, through the cleavage of S–N bond in the SMX due to oxidation by •OH radical that leads to the formation of end-product denoted by C9 with an m/z value of 99.20.

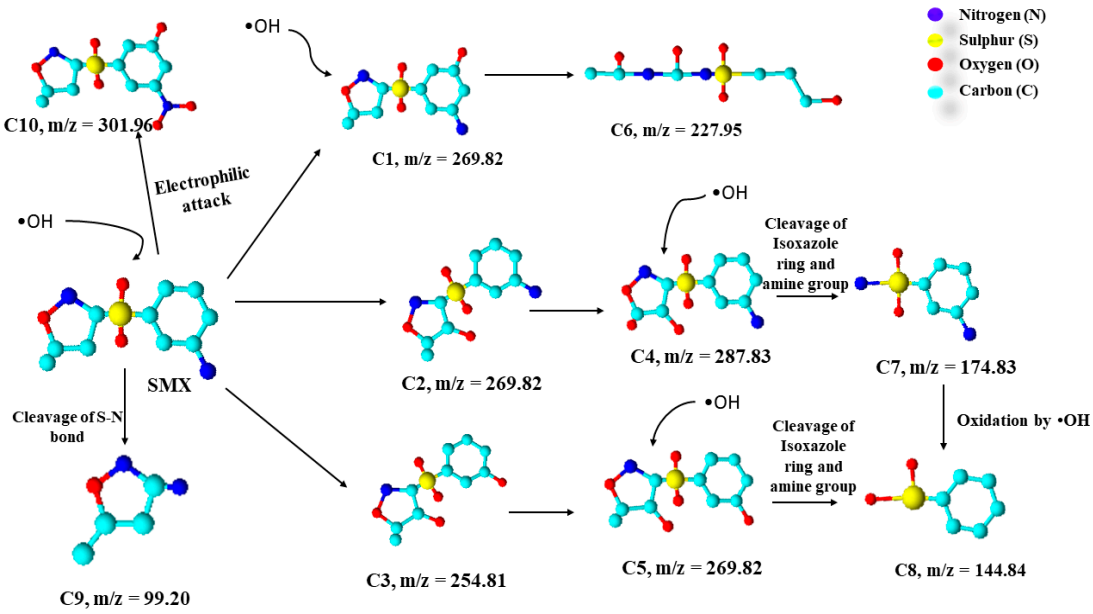

Figure 10. Photochemical degradation mechanism of SMX in water (adapted from [87,88] Copyright Year 2016 and 2017, Journal of Hazardous Materials and Chemosphere with permission License numbers: 5191250118976 and 5191390107382).

Besides this, a separate comparison has been discussed with respect to the synthesis techniques used for the synthesis of AC, biochar, reduced graphene oxide (rGO), and metal-doped TiO_2 based photocatalysts and the effect of the various synthesis methods on the surface area and removal efficiency of various antibiotics (Table 2). It can be observed from the table that various synthesis methods, such as sol–gel, solvothermal, ultrasound method, thermal treatment, and hydrothermal methods, were used to synthesize AC, biochar, and metal-doped TiO_2 photocatalysts. Among the reported methods, it was found that the AC-based TiO_2 composite developed through the sol–gel method showed the highest removal efficiency of antibiotics (Tetracycline), followed by the rGO/TiO_2 composite developed through the hydrothermal method. Subsequently, the BC/Zn/TiO_2 and BiOBr/BC composites developed through the solvothermal method have shown high antibiotic removal efficiency of 96.8 and 92%, respectively. Conversely, the least organic pollutant removal was shown by the BC-TiO_2 composite developed through the ultrasound-promoted wet impregnation method. Moreover, an interesting result was observed that the photocatalytic degradation of antibiotics was not much influenced by the surface area of the photocatalyst; rather, it depends on the synthesis method, the doping material being utilized for the development of the photocatalyst, as well as the pore volume of the photocatalyst. As far as the synthesis cost is concerned concerning the efficiency of the photocatalysts, it is beyond the scope of the present work. However, based on the technical methods and efficiency of the processes, it can be said that the sol–gel and hydrothermal are the most efficient and suitable methods to synthesize nanoscale photocatalysts having very high efficiency for the degradation of antibiotics in water.

Table 2. Comparison of synthesis methods on the properties of carbon-based TiO_2 nanocomposites and the removal efficiency of antibiotics.

S. No.	Composite Material	Synthesis Method Used	BET Surface Area (m^2/g)	Pore Volume (cc/g)	Targeted Antibiotic	Mechanism of Removal	Removal Efficiency	References
1	AC/TiO_2	Sol–gel	129	0.30	Tetracycline	Photocatalysis	~97%	[102]
2	$BC/Zn/TiO_2$	Solvothermal	435	-	acetaminophen	Photocatalysis	92%	[103]
3	BC-BiOCl	One step hydrolysis	3,546	0.011	Tetracycline	Photocatalysis	60.3%	[104]
4	BC-TiO_2	Ultrasound promoted wet impregnation	399	-	Phenol	Photocatalysis	64.1% (UV light) 55667733.6% (Visible light)	[78]
5	Magnetic BC/TiO_2	Solvothermal	-	-	Sulfadiazine	Photocatalysis	~88%	[105]
6	TiO_2/rGO	Hydrothermal	48.09	-	Sulfamethoxazole	Photocatalysis	~90%	[106]
7	rGO/TiO_2/Na Alginate	Hydrothermal	-	-	Azithromycin	Photocatalysis	~99%	[81]
8	$Bi/Bi_2O_3/BC$	Thermal method	338.2	0.161	Estrone	Photocatalysis	~90%	[107]
9	BioBr/BC	Solvothermal	-	-	Ciprofloxacin	Photocatalysis	96.8%	[108]
10	$CuWO_4/BC$	Hydrothermal	6.8104	-	Ciprofloxacin	Photocatalysis	97%	[109]

7. Conclusions and Future Prospective

In the current perspective, the following conclusions can be deduced from the review:

(1) The use of a biochar-supported TiO_2 composite for the photocatalytic degradation of antibiotics is an attractive method due to its high efficiency and low cost of operation compared to the existing treatment processes.

(2) The integration of biochar with the TiO_2 nanoparticles increased photocatalytic degradation of SMX by increasing its photocatalytic response in the UV-visible range (200–700 nm) and the interaction of SMX with the TiO_2 through the adsorption onto the biochar/TiO_2 composite interface.

(3) The biochar-supported TiO_2 composite can remove up to more than 95% of SMX in the aqueous solution within the UV range and up to 75% efficiency in the visible range.

(4) Unlike the doped photocatalyst, the biochar-supported TiO_2 nanoparticles degrade the sulfamethoxazole both by adsorption and photocatalysis process and could also be used for the photocatalytic degradation of other antibiotics.

(5) The •OH free radical is the prime key component that degrades the sulfamethoxazole through the oxidation or reduction process.

In the future, more studies focusing on the application of biochar-supported TiO_2 composites for the photocatalytic degradation of antibiotics in the natural water stream under sunlight irradiation are required. Moreover, future studies should pay more attention to enhancing the adsorption capacity of biochar by doping it with certain metal or non-metal elements to increase the adsorption of anionic antibiotics onto the biochar-TiO_2 surface to increase the photocatalytic degradation. Additionally, more studies are required focusing on the photocatalytic degradation of SMX using a biochar/TiO_2 composite in real water under open sunlight as very limited studies are available delineating the photocatalytic degradation mechanism of SMX using the biochar/TiO_2 composite.

Author Contributions: S.C.: conceptualization, data curation, and writing—original draft; P.J.: project administration, supervision, and writing—review and editing; I.M.: conceptualization, data curation, and writing—original draft; A.K.T.: data curation and formal analysis; M.B.: data curation and formal analysis; A.D.N.: data curation and formal analysis; F.O.: project administration, supervision, and writing—review and editing. All authors have read and agreed to the published version of the manuscript.

Funding: This review received no external funding.

Institutional Review Board Statement: Not applicable.

Informed Consent Statement: Not applicable.

Data Availability Statement: Not applicable.

Conflicts of Interest: The authors declare no conflict of interest.

References

1. Gebre, S.L.; Cattrysse, D.; Van Orshoven, J. Multi-criteria decision-making methods to address water allocation problems: A systematic review. *Water* **2021**, *13*, 125. [CrossRef]
2. Santy, S.; Mujumdar, P.; Bala, G. Potential Impacts of Climate and Land Use Change on the Water Quality of Ganga River around the Industrialized Kanpur Region. *Sci. Rep.* **2020**, *10*, 9107. [CrossRef]
3. Al Maliki, A.A.; Abbass, Z.D.; Hussain, H.M.; Al-Ansari, N. Assessment of the groundwater suitability for irrigation near Al Kufa City and preparing the final water quality maps using spatial distribution tools. *Environ. Earth Sci.* **2020**, *79*, 330. [CrossRef]
4. Usman, M.; Farooq, M.; Hanna, K. Environmental side effects of the injudicious use of antimicrobials in the era of COVID-19. *Sci. Total Environ.* **2020**, *745*, 141053. [CrossRef]
5. Lucien, M.A.B.; Canarie, M.F.; Kilgore, P.E.; Jean-Denis, G.; Fénélon, N.; Pierre, M.; Cerpa, M.; Joseph, G.A.; Maki, G.; Zervos, M.J.; et al. Antibiotics and antimicrobial resistance in the COVID-19 era: Perspective from resource-limited settings. *Int. J. Infect. Dis.* **2021**, *104*, 250–254. [CrossRef] [PubMed]
6. Chow, L.K.M.; Ghaly, T.M.; Gillings, M.R. A survey of sub-inhibitory concentrations of antibiotics in the environment. *J. Environ. Sci.* **2021**, *99*, 21–27. [CrossRef] [PubMed]
7. Harrower, J.; McNaughtan, M.; Hunter, C.; Hough, R.; Zhang, Z.; Helwig, K. Chemical Fate and Partitioning Behaviour of Antibiotics in the Aquatic Environment—A Review. *Environ. Toxicol. Chem.* **2021**, 1–24. [CrossRef]
8. Zainab, S.M.; Junaid, M.; Rehman, M.Y.A.; Lv, M.; Yue, L.; Xu, N.; Malik, R.N. First insight into the occurrence, spatial distribution, sources, and risks assessment of antibiotics in groundwater from major urban-rural settings of Pakistan. *Sci. Total Environ.* **2021**, *791*, 148298. [CrossRef] [PubMed]
9. Li, D.; Shao, H.; Huo, Z.; Xie, N.; Gu, J.; Xu, G. Typical antibiotics in the receiving rivers of direct-discharge sources of sewage across Shanghai: Occurrence and source analysis. *RSC Adv.* **2021**, *11*, 21579–21587. [CrossRef]
10. Xu, B.; Mao, D.; Luo, Y.; Xu, L. Sulfamethoxazole biodegradation and biotransformation in the water-sediment system of a natural river. *Bioresour. Technol.* **2011**, *102*, 7069–7076. [CrossRef]
11. Drori, Y.; Aizenshtat, Z.; Chefetz, B. Sorption-Desorption Behavior of Atrazine in Soils Irrigated with Reclaimed Wastewater. *Soil Sci. Soc. Am. J.* **2005**, *69*, 1703–1710. [CrossRef]
12. Steven Leeder, J.; Dosch, H.M.; Spielberg, S.P. Cellular toxicity of sulfamethoxazole reactive metabolites-I. Inhibition of intracellular esterase activity prior to cell death. *Biochem. Pharmacol.* **1991**, *41*, 567–574. [CrossRef]
13. Jesús García-Galán, M.; Díaz-Cruz, M.S.; Barceló, D. Identification and determination of metabolites and degradation products of sulfonamide antibiotics. *Trends Anal. Chem.* **2008**, *27*, 1008–1022. [CrossRef]
14. Tamtam, F.; Mercier, F.; Le, B.; Eurin, J.; Tuc, Q.; Clément, M.; Chevreuil, M.; Pierre, U.; Ephe, C.; Sisyphe, U.M.R.; et al. Occurrence and fate of antibiotics in the Seine River in various hydrological conditions. *Sci. Total Environ.* **2007**, *93*, 84–95. [CrossRef]
15. Luo, Y.; Mao, D.; Rysz, M.; Zhou, Q.; Zhang, H.; Xu, L.; Alvarez, P. Trends in antibiotic resistance genes occurrence in the Haihe River, China. *Environ. Sci. Technol.* **2010**, *44*, 7220–7225. [CrossRef]
16. Moreno-González, R.; Rodríguez-Mozaz, S.; Gros, M.; Pérez-Cánovas, E.; Barceló, D.; León, V.M. Input of pharmaceuticals through coastal surface watercourses into a Mediterranean lagoon (Mar Menor, SE Spain): Sources and seasonal variations. *Sci. Total Environ.* **2014**, *490*, 59–72. [CrossRef] [PubMed]
17. Cetecioglu, Z.; Ince, B.; Gros, M.; Rodriguez-Mozaz, S.; Barceló, D.; Ince, O.; Orhon, D. Biodegradation and reversible inhibitory impact of sulfamethoxazole on the utilization of volatile fatty acids during anaerobic treatment of pharmaceutical industry wastewater. *Sci. Total Environ.* **2015**, *536*, 667–674. [CrossRef]
18. Song, L.; Li, L.; Yang, S.; Lan, J.; He, H.; McElmurry, S.P.; Zhao, Y. Sulfamethoxazole, tetracycline and oxytetracycline and related antibiotic resistance genes in a large-scale landfill, China. *Sci. Total Environ.* **2016**, *551–552*, 9–15. [CrossRef]
19. Yang, Q.; Chen, D.; Chu, L.; Wang, J. Enhancement of ionizing radiation-induced catalytic degradation of antibiotics using Fe/C nanomaterials derived from Fe-based MOFs. *J. Hazard. Mater.* **2020**, *389*, 122148. [CrossRef]

20. Kumar Subramani, A.; Rani, P.; Wang, P.H.; Chen, B.Y.; Mohan, S.; Chang, C.T. Performance assessment of the combined treatment for oxytetracycline antibiotics removal by sonocatalysis and degradation using Pseudomonas aeruginosa. *J. Environ. Chem. Eng.* **2019**, *7*, 103215. [CrossRef]
21. Liu, Q.; Li, M.; Liu, X.; Zhang, Q.; Liu, R.; Wang, Z.; Shi, X.; Quan, J. Removal of sulfamethoxazole and trimethoprim from reclaimed water and the biodegradation mechanism. *Front. Environ. Sci. Eng.* **2018**, *12*, 6. [CrossRef]
22. Shang, Y.; Chen, C.; Zhang, P.; Yue, Q.; Li, Y.; Gao, B.; Xu, X. Removal of sulfamethoxazole from water via activation of persulfate by Fe_3C@NCNTs including mechanism of radical and nonradical process. *Chem. Eng. J.* **2019**, *375*, 122004. [CrossRef]
23. Tian, Y.; Gao, B.; Morales, V.L.; Chen, H.; Wang, Y.; Li, H. Removal of sulfamethoxazole and sulfapyridine by carbon nanotubes in fixed-bed columns. *Chemosphere* **2013**, *90*, 2597–2605. [CrossRef] [PubMed]
24. Wang, W.L.; Wu, Q.Y.; Huang, N.; Xu, Z.B.; Lee, M.Y.; Hu, H.Y. Potential risks from UV/H_2O_2 oxidation and UV photocatalysis: A review of toxic, assimilable, and sensory-unpleasant transformation products. *Water Res.* **2018**, *141*, 109–125. [CrossRef] [PubMed]
25. Salimi, M.; Esrafili, A.; Gholami, M.; Jonidi Jafari, A.; Rezaei Kalantary, R.; Farzadkia, M.; Kermani, M.; Sobhi, H.R. Contaminants of emerging concern: A review of new approach in AOP technologies. *Environ. Monit. Assess.* **2017**, *189*, 414. [CrossRef]
26. Mirzaei, A.; Yerushalmi, L.; Chen, Z.; Haghighat, F. Photocatalytic degradation of sulfamethoxazole by hierarchical magnetic ZnO@g-C_3N_4: RSM optimization, kinetic study, reaction pathway and toxicity evaluation. *J. Hazard. Mater.* **2018**, *359*, 516–526. [CrossRef]
27. Bayarri, B.; Gime, J.; Costa, J.; Abella, M.N. Photocatalytic degradation of sulfamethoxazole in aqueous suspension of TiO_2. *Appl. Catal. B Environ.* **2007**, *74*, 233–241. [CrossRef]
28. Yuan, R.; Zhu, Y.; Zhou, B.; Hu, J. Photocatalytic oxidation of sulfamethoxazole in the presence of TiO_2: Effect of matrix in aqueous solution on decomposition mechanisms. *Chem. Eng. J.* **2019**, *359*, 1527–1536. [CrossRef]
29. Elmolla, E.S.; Chaudhuri, M. Photocatalytic degradation of amoxicillin, ampicillin and cloxacillin antibiotics in aqueous solution using UV/TiO_2 and UV/H_2O_2/TiO_2 photocatalysis. *Desalination* **2010**, *252*, 46–52. [CrossRef]
30. Dong, H.; Zeng, G.; Tang, L.; Fan, C. An overview on limitations of TiO_2-based particles for photocatalytic degradation of organic pollutants and the corresponding countermeasures. *Water Res.* **2015**, *79*, 128–146. [CrossRef]
31. Zhang, J.; Wu, Y.; Xing, M.; Ahmed, S.; Leghari, K.; Sajjad, S. Development of modified N doped TiO_2 photocatalyst with metals, nonmetals and metal oxides. *Energy Environ. Sci.* **2010**, *3*, 715–726. [CrossRef]
32. Hao, H.; Zhang, J. Microporous and Mesoporous Materials The study of Iron (III) and nitrogen co-doped mesoporous TiO_2 photocatalysts: Synthesis, characterization and activity. *Microporous Mesoporous Mater.* **2009**, *121*, 52–57. [CrossRef]
33. Koo, Y.; Littlejohn, G.; Collins, B.; Yun, Y.; Shanov, V.N.; Schulz, M.; Pai, D.; Sankar, J. Synthesis and characterization of Ag–TiO_2–CNT nanoparticle composites with high photocatalytic activity under artificial light. *Compos. Part B* **2014**, *57*, 105–111. [CrossRef]
34. Kasemets, K.; Ivask, A.; Dubourguier, H.; Kahru, A. Toxicology of nanoparticles of ZnO, CuO and TiO_2 to yeast *Saccharomyces cerevisiae*. *Toxicol. In Vitro* **2009**, *23*, 1116–1122. [CrossRef] [PubMed]
35. Shan, R.; Lu, L.; Gu, J.; Zhang, Y.; Yuan, H. Photocatalytic degradation of methyl orange by Ag/TiO_2/biochar composite catalysts in aqueous solutions. *Mater. Sci. Semicond. Process.* **2020**, *114*, 105088. [CrossRef]
36. Chandra, S.; Bhattacharya, J. Influence of temperature and duration of pyrolysis on the property heterogeneity of rice straw biochar and optimization of pyrolysis conditions for its application in soils. *J. Clean. Prod.* **2019**, *215*, 1123–1139. [CrossRef]
37. Kappler, A.; Wuestner, M.L.; Ruecker, A.; Harter, J.; Halama, M.; Behrens, S. Biochar as an Electron Shuttle between Bacteria and Fe (III) Minerals. *Environ. Sci. Technol. Lett.* **2014**, *1*, 339–344. [CrossRef]
38. Kim, J.R.; Kan, E. Heterogeneous photocatalytic degradation of sulfamethoxazole in water using a biochar-supported TiO_2 photocatalyst. *J. Environ. Manag.* **2016**, *180*, 94–101. [CrossRef]
39. Xie, X.; Li, S.; Zhang, H.; Wang, Z.; Huang, H. Promoting charge separation of biochar-based Zn-TiO_2/pBC in the presence of ZnO for efficient sulfamethoxazole photodegradation under visible light irradiation. *Sci. Total Environ.* **2019**, *659*, 529–539. [CrossRef]
40. Avramiotis, E.; Frontistis, Z.; Manariotis, I.D.; Vakros, J.; Mantzavinos, D. Oxidation of sulfamethoxazole by rice husk biochar-activated persulfate. *Catalysts* **2021**, *11*, 850. [CrossRef]
41. Sun, S.; Yao, H.; Li, X.; Deng, S.; Zhao, S.; Zhang, W. Enhanced degradation of sulfamethoxazole (SMX) in toilet wastewater by photo-fenton reactive membrane filtration. *Nanomaterials* **2020**, *10*, 180. [CrossRef]
42. Liu, Z.; Hu, W.; Zhang, H.; Wang, H.; Sun, P. Enhanced degradation of sulfonamide antibiotics by UV irradiation combined with persulfate. *Processes* **2021**, *9*, 226. [CrossRef]
43. Vignati, D.A.L.; Lofrano, G.; Libralato, G.; Guida, M.; Siciliano, A.; Carraturo, F.; Carotenuto, M. Photocatalytic ZnO-assisted degradation of spiramycin in urban wastewater: Degradation kinetics and toxicity. *Water* **2021**, *13*, 1051. [CrossRef]
44. Zhu, Z.; Han, S.; Cao, Y.; Jiang, J. Synthesis of a Novel Photocatalyst MVO_4/g-C_3N_4 (M = La, Gd) with Better Photocatalytic Activity for Tetracycline Hydrochloride Degradation under Visible-Light Irradiation. *Crystals* **2021**, *11*, 756. [CrossRef]
45. Anh, H.Q.; Le, T.P.Q.; Da Le, N.; Lu, X.X.; Duong, T.T.; Garnier, J.; Rochelle-Newall, E.; Zhang, S.; Oh, N.H.; Oeurng, C.; et al. Antibiotics in surface water of East and Southeast Asian countries: A focused review on contamination status, pollution sources, potential risks, and future perspectives. *Sci. Total Environ.* **2021**, *764*. [CrossRef]

46. Le, T.X.; Munekage, Y. Residues of selected antibiotics in water and mud from shrimp ponds in mangrove areas in Viet Nam. *Mar. Pollut. Bull.* **2004**, *49*, 922–929. [CrossRef] [PubMed]
47. Shimizu, A.; Takada, H.; Koike, T.; Takeshita, A.; Saha, M.; Rinawati; Nakada, N.; Murata, A.; Suzuki, T.; Suzuki, S.; et al. Ubiquitous occurrence of sulfonamides in tropical Asian waters. *Sci. Total Environ.* **2013**, *452–453*, 108–115. [CrossRef]
48. Tran, N.H.; Hoang, L.; Nghiem, L.D.; Nguyen, N.M.H.; Ngo, H.H.; Guo, W.; Trinh, Q.T.; Mai, N.H.; Chen, H.; Nguyen, D.D.; et al. Occurrence and risk assessment of multiple classes of antibiotics in urban canals and lakes in Hanoi, Vietnam. *Sci. Total Environ.* **2019**, *692*, 157–174. [CrossRef]
49. Sim, W.J.; Lee, J.W.; Lee, E.S.; Shin, S.K.; Hwang, S.R.; Oh, J.E. Occurrence and distribution of pharmaceuticals in wastewater from households, livestock farms, hospitals and pharmaceutical manufactures. *Chemosphere* **2011**, *82*, 179–186. [CrossRef] [PubMed]
50. Kim, J.-P.; Jin, D.R.; Lee, W.; Chae, M.; Park, J. Occurrence and Removal of Veterinary Antibiotics in Livestock Wastewater Treatment Plants, South Korea. *Processes* **2020**, *8*, 720. [CrossRef]
51. Lien, L.T.Q.; Hoa, N.Q.; Chuc, N.T.K.; Thoa, N.T.M.; Phuc, H.D.; Diwan, V.; Dat, N.T.; Tamhankar, A.J.; Lundborg, C.S. Antibiotics in wastewater of a rural and an urban hospital before and after wastewater treatment, and the relationship with antibiotic use-a one year study from Vietnam. *Int. J. Environ. Res. Public Health* **2016**, *13*, 588. [CrossRef]
52. Jiang, H.; Zhang, D.; Xiao, S.; Geng, C.; Zhang, X. Occurrence and sources of antibiotics and their metabolites in river water, WWTPs, and swine wastewater in Jiulongjiang River basin, south China. *Environ. Sci. Pollut. Res.* **2013**, *20*, 9075–9083. [CrossRef] [PubMed]
53. Wu, D.; Huang, Z.; Yang, K.; Graham, D.; Xie, B. Relationships between Antibiotics and Antibiotic Resistance Gene Levels in Municipal Solid Waste Leachates in Shanghai, China. *Environ. Sci. Technol.* **2015**, *49*, 4122–4128. [CrossRef]
54. Shi, Y.; Liu, J.; Zhuo, L.; Yan, X. Antibiotics in wastewater from multiple sources and surface water of the Yangtze River in Chongqing in China. *Environ. Monit. Assess.* **2020**, *192*, 1–13. [CrossRef] [PubMed]
55. City, M.; Vo, T.; Bui, X.; Cao, N.; Luu, V. Investigation of antibiotics in health care wastewater in Ho Chi. *Environ. Monit. Assess.* **2016**, *188*, 1–9. [CrossRef]
56. Anh, H.; Ha, N.; Tung, H.; Thuong, T.; Viet, H.; Pham, V.C.; Berg, M.; Giger, W.; Alder, A.C. Occurrence, fate and antibiotic resistance of fluoroquinolone antibacterials in hospital wastewaters in Hanoi, Vietnam. *Chemosphere* **2008**, *72*, 968–973. [CrossRef]
57. Thai, P.K.; Ky, L.X.; Binh, V.N.; Nhung, P.H.; Nhan, P.T.; Hieu, N.Q.; Dang, N.T.T.; Tam, N.K.B.; Anh, N.T.K. Occurrence of antibiotic residues and antibiotic-resistant bacteria in effluents of pharmaceutical manufacturers and other sources around Hanoi, Vietnam. *Sci. Total Environ.* **2018**, *645*, 393–400. [CrossRef]
58. Avisar, D.; Lester, Y.; Ronen, D. Sulfamethoxazole contamination of a deep phreatic aquifer. *Sci. Total Environ.* **2009**, *407*, 4278–4282. [CrossRef]
59. Çalişkan, E.; Göktürk, S. Adsorption characteristics of sulfamethoxazole and metronidazole on activated carbon. *Sep. Sci. Technol.* **2010**, *45*, 244–255. [CrossRef]
60. Dirany, A.; Efremova Aaron, S.; Oturan, N.; Sirés, I.; Oturan, M.A.; Aaron, J.J. Study of the toxicity of sulfamethoxazole and its degradation products in water by a Thaibioluminescence method during application of the electro-Fenton treatment. *Anal. Bioanal. Chem.* **2011**, *400*, 353–360. [CrossRef]
61. Prasannamedha, G.; Kumar, P.S. A review on contamination and removal of sulfamethoxazole from aqueous solution using cleaner techniques: Present and future perspective. *J. Clean. Prod.* **2020**, *250*, 119553. [CrossRef]
62. Białk-bieli, A.; Stolte, S.; Matzke, M.; Fabia, A.; Maszkowska, J.; Kołodziejska, M.; Liberek, B.; Stepnowski, P.; Kumirska, J. Hydrolysis of sulphonamides in aqueous solutions. *J. Hazard. Mater.* **2012**, *222*, 264–274. [CrossRef] [PubMed]
63. Thomsen, A.; McArdell, C.S.; Joss, A.; Giger, W. Occurrence and Sorption Behavior of Sulfonamides, Macrolides, and Trimethoprim in Activated Sludge Treatment. *Environ. Sci. Technol.* **2005**, *39*, 3981–3989.
64. Długosz, M.; Zmudzki, P.; Kwiecień, A.; Szczubiałka, K.; Krzek, J.; Nowakowska, M. Photocatalytic degradation of sulfamethoxazole in aqueous solution using a floating TiO_2-expanded perlite photocatalyst. *J. Hazard. Mater.* **2015**, *298*, 146–153. [CrossRef]
65. Jing, H.; Li, Y.; Wang, X. Environmental Science Water Research & Technology supported $Mg(OH)_2$/bentonite composite. *Environ. Sci. Water Res. Technol.* **2019**, *5*, 931–943. [CrossRef]
66. Kitano, M.; Matsuoka, M.; Ueshima, M.; Anpo, M. Recent developments in titanium oxide-based photocatalysts. *Appl. Catal. A Gen.* **2007**, *325*, 1–14. [CrossRef]
67. Shi, M.; Shen, J.; Ma, H.; Li, Z.; Lu, X.; Li, N.; Ye, M. Physicochemical and Engineering Aspects Preparation of graphene–TiO_2 composite by hydrothermal method from peroxotitanium acid and its photocatalytic properties. *Colloids Surf. A Physicochem. Eng. Asp.* **2012**, *405*, 30–37. [CrossRef]
68. Andriantsiferana, C.; Mohamed, E.F.; Delmas, H. Photocatalytic degradation of an azo-dye on TiO_2/activated carbon composite material. *Environ. Technol.* **2014**, *35*, 355–363. [CrossRef] [PubMed]
69. Dorraj, M.; Alizadeh, M.; Asrina, N.; Jefrey, W. Enhanced visible-light photocatalytic activity of copper-doped titanium oxide–zinc oxide heterojunction for methyl orange degradation. *Appl. Surf. Sci.* **2017**, *414*, 251–261. [CrossRef]
70. Lu, L.; Shan, R.; Shi, Y.; Wang, S.; Yuan, H. A novel TiO_2/biochar composite catalysts for photocatalytic degradation of methyl orange. *Chemosphere* **2019**, *222*, 391–398. [CrossRef] [PubMed]
71. Matos, J.; Herna, J.C.; Atienzar, P.; Garcı, H. Nanocrystalline carbon–TiO_2 hybrid hollow spheres as possible electrodes for solar cells. *Carbon* **2013**, *53*, 169–181. [CrossRef]

72. Matos, J.; Corma, A. General Selective phenol hydrogenation in aqueous phase on Pd-based catalysts supported on hybrid TiO_2-carbon materials. *Appl. Catal. A Gen.* **2011**, *404*, 103–112. [CrossRef]
73. Mian, M.; Liu, G. Recent progress in biochar-supported photocatalysts: Synthesis, role of biochar, and applications. *RSC Adv.* **2018**, *8*, 14237–14248. [CrossRef]
74. Yin, S.; Zhang, Q.; Saito, F.; Sato, T. Preparation of visible light-activated titania photocatalyst by mechanochemical method. *Chem. Lett.* **2003**, *32*, 358–359. [CrossRef]
75. Mian, M.; Liu, G. Sewage sludge-derived TiO_2/Fe/Fe_3C-biochar composite as an efficient heterogeneous catalyst for degradation of methylene blue. *Chemosphere* **2019**, *215*, 110–114. [CrossRef] [PubMed]
76. Silvestri, S.; Stefanello, N.; Sulkovski, A.; Luiz, E. Preparation of TiO_2 supported on MDF biochar for simultaneous removal of methylene blue by adsorption and photocatalysis. *J. Chem. Technol. Biotechnol.* **2019**, *95*, 2723–2729. [CrossRef]
77. Rismanchian, M.; Golbabaei, F.; Mortazavi, Y.; Pourtaghi, G.; Rahimi Foroushani, A.; Nassiri, P. A Comparative Evaluation of TiO_2 Suspension Coating Techniques: A Novel Technique to Achieve Optimal Thickness and Uniformity of Photocatalytic Film. *Int. J. Photoenergy* **2012**, *2012*, 634802. [CrossRef]
78. Lisowski, P.; Colmenares, J.C.; Mašek, O. Dual functionality of TiO_2/biochar hybrid materials: Photocatalytic phenol degradation in liquid phase and selective oxidation of methanol in gas phase. *ACS Sustain. Chem. Eng.* **2017**, *5*, 6274–6287. [CrossRef]
79. Zhang, H.; Chen, C.; Gray, E.M.; Boyd, S.E. Effect of feedstock and pyrolysis temperature on properties of biochar governing end-use efficacy. *Biomass Bioenergy* **2017**, *105*, 136–146. [CrossRef]
80. Pamphile, N.; Xuejiao, L.; Guangwei, Y.; Yin, W. Synthesis of a novel core-shell-structure activated carbon material and its application in sulfamethoxazole adsorption. *J. Hazard. Mater.* **2019**, *368*, 602–612. [CrossRef]
81. Nielsen, L.; Biggs, M.J.; Skinner, W.; Bandosz, T.J. The effects of activated carbon surface features on the reactive adsorption of carbamazepine and sulfamethoxazole. *Carbon* **2014**, *80*, 419–432. [CrossRef]
82. Moral-Rodríguez, A.I.; Leyva-Ramos, R.; Ocampo-Pérez, R.; Mendoza-Barron, J.; Serratos-Alvarez, I.N.; Salazar-Rabago, J.J. Removal of ronidazole and sulfamethoxazole from water solutions by adsorption on granular activated carbon: Equilibrium and intraparticle diffusion mechanisms. *Adsorption* **2016**, *22*, 89–103. [CrossRef]
83. Nam, S.W.; Jung, C.; Li, H.; Yu, M.; Flora, J.R.V.; Boateng, L.K.; Her, N.; Zoh, K.D.; Yoon, Y. Adsorption characteristics of diclofenac and sulfamethoxazole to graphene oxide in aqueous solution. *Chemosphere* **2015**, *136*, 20–26. [CrossRef]
84. Rostamian, R.; Behnejad, H. A comparative adsorption study of sulfamethoxazole onto graphene and graphene oxide nanosheets through equilibrium, kinetic and thermodynamic modelling. *Process Saf. Environ. Prot.* **2016**, *102*, 20–29. [CrossRef]
85. Liu, S.; Pan, M.; Feng, Z.; Qin, Y.; Wang, Y.; Tan, L.; Sun, T. Ultra-high adsorption of tetracycline antibiotics on garlic skin-derived porous biomass carbon with high surface area. *New J. Chem.* **2020**, *44*, 1097–1106. [CrossRef]
86. Cuerda-Correa, E.M.; Alexandre-Franco, M.F.; Fern, C. Advanced Oxidation Processes for the Removal of Antibiotics from Water. An Overview. *Water* **2020**, *12*, 102. [CrossRef]
87. Gong, H.; Chu, W. Determination and toxicity evaluation of the generated products in sulfamethoxazole degradation by UV/$CoFe_2O_4$/TiO_2. *J. Hazard. Mater.* **2016**, *314*, 197–203. [CrossRef]
88. Zhang, H.; Wang, Z.; Li, R.; Guo, J.; Li, Y.; Zhu, J.; Xie, X. TiO_2 supported on reed straw biochar as an adsorptive and photocatalytic composite for the efficient degradation of sulfamethoxazole in aqueous matrices. *Chemosphere* **2017**, *185*, 351–360. [CrossRef]
89. Schwarz, P.F.; Turro, N.J.; Bossmann, S.H.; Braun, A.M.; Abdel Wahab, A.M.A.; Dürr, H. A new method to determine the generation of hydroxyl radicals in illuminated TiO_2 suspensions. *J. Phys. Chem. B* **1997**, *101*, 7127–7134. [CrossRef]
90. Gar Alalm, M.; Tawfik, A.; Ookawara, S. Enhancement of photocatalytic activity of TiO_2 by immobilization on activated carbon for degradation of pharmaceuticals. *J. Environ. Chem. Eng.* **2016**, *4*, 1929–1937. [CrossRef]
91. Bems, B.; Jentoft, F.C.; Schlögl, R. Photoinduced decomposition of nitrate in drinking water in the presence of titania and humic acids. *Appl. Catal. B Environ.* **1999**, *20*, 155–163. [CrossRef]
92. Hassani, A.; Khataee, A.; Karaca, S.; Karaca, C.; Gholami, P. Sonocatalytic degradation of ciprofloxacin using synthesized TiO_2 nanoparticles on montmorillonite. *Ultrason. Sonochem.* **2017**, *35*, 251–262. [CrossRef]
93. Song, C.; Wang, L.; Ren, J.; Lv, B.; Sun, Z.; Yan, J.; Li, X.; Liu, J. Comparative study of diethyl phthalate degradation by UV/H_2O_2 and UV/TiO_2: Kinetics, mechanism, and effects of operational parameters. *Environ. Sci. Pollut. Res.* **2016**, *23*, 2640–2650. [CrossRef] [PubMed]
94. Zhang, Q.; Rao, G.; Rogers, J.; Zhao, C.; Liu, L.; Li, Y. Novel anti-fouling Fe_2O_3/TiO_2 nanowire membranes for humic acid removal from water. *Chem. Eng. J.* **2015**, *271*, 180–187. [CrossRef]
95. Nawaz, M.; Khan, A.A.; Hussain, A.; Jang, J.; Jung, H.Y.; Lee, D.S. Reduced graphene oxide−TiO_2/sodium alginate 3-dimensional structure aerogel for enhanced photocatalytic degradation of ibuprofen and sulfamethoxazole. *Chemosphere* **2020**, *261*, 127702. [CrossRef] [PubMed]
96. Awfa, D.; Ateia, M.; Fujii, M.; Yoshimura, C. Novel Magnetic Carbon Nanotube-TiO_2 Composites for Solar Light Photocatalytic Degradation of Pharmaceuticals in the Presence of Natural Organic Matter. *J. Water Process Eng.* **2019**, *31*, 100836. [CrossRef]
97. Alfred, M.O.; Omorogie, M.O.; Bodede, O.; Moodley, R.; Ogunlaja, A.; Adeyemi, O.G.; Günter, C.; Taubert, A.; Iermak, I.; Eckert, H.; et al. Solar-active clay-TiO_2 nanocomposites prepared via biomass assisted synthesis: Efficient removal of ampicillin, sulfamethoxazole and artemether from water. *Chem. Eng. J.* **2020**, *398*, 125544. [CrossRef]

98. Evgenidou, E.; Chatzisalata, Z.; Tsevis, A.; Bourikas, K.; Torounidou, P.; Sergelidis, D.; Koltsakidou, A.; Lambropoulou, D.A. Photocatalytic degradation of a mixture of eight antibiotics using Cu-modified TiO_2 photocatalysts: Kinetics, mineralization, antimicrobial activity elimination and disinfection. *J. Environ. Chem. Eng.* **2021**, *9*, 105295. [CrossRef]
99. Asha, R.C.; Yadav, M.S.P.; Kumar, M. Sulfamethoxazole Removal in Membrane-Photocatalytic Reactor System—Experimentation and Modelling. *Environ. Technol.* **2019**, *40*, 1607–1704. [CrossRef]
100. Ricardo, P.; Pretto, P.; Palácio, S.M.; de Campos, É.A.; Pazini, C.R.; Veit, M.T. Sulfamethoxazole photocatalytic degradation in a continuous flow reactor using artificial radiation. *J. Environ. Chem. Eng.* **2018**, *6*, 1926–1933. [CrossRef]
101. Ling, C.; Yue, C.; Yuan, R.; Qiu, J.; Liu, F.; Zhu, J. Enhanced removal of sulfamethoxazole by a novel composite of TiO_2 nanocrystals in situ wrapped-Bi_2O_4 microrods under simulated solar irradiation. *Chem. Eng. J.* **2020**, *384*, 123278. [CrossRef]
102. Martins, A.C.; Cazetta, A.L.; Pezoti, O.; Souza, J.R.B.; Zhang, T.; Pilau, E.J.; Asefa, T.; Almeida, V.C. Sol-gel synthesis of new TiO_2/activated carbon photocatalyst and its application for degradation of tetracycline. *Ceram. Int.* **2017**, *43*, 4411–4418. [CrossRef]
103. Peñas-Garzón, M.; Gómez-Avilés, A.; Bedia, J.; Rodriguez, J.J.; Belver, C. Effect of activating agent on the properties of TiO_2/activated carbon heterostructures for solar photocatalytic degradation of acetaminophen. *Materials* **2019**, *12*, 378. [CrossRef] [PubMed]
104. Liu, M.Y.; Zheng, Y.F.; Song, X.C. Biomass Assisted Synthesis of 3D Hierarchical Structure BiOX(X Cl, Br)-(CMC) with Enhanced Photocatalytic Activity. *J. Nanosci. Nanotechnol.* **2019**, *19*, 5287–5294. [CrossRef] [PubMed]
105. Silva, C.P.; Pereira, D.; Calisto, V.; Martins, M.A.; Otero, M.; Esteves, V.I.; Lima, D.L.D. Biochar-TiO_2 magnetic nanocomposites for photocatalytic solar-driven removal of antibiotics from aquaculture effluents. *J. Environ. Manag.* **2021**, *294*, 112937. [CrossRef]
106. Karaolia, P.; Michael-Kordatou, I.; Hapeshi, E.; Drosou, C.; Bertakis, Y.; Christofilos, D.; Armatas, G.S.; Sygellou, L.; Schwartz, T.; Xekoukoulotakis, N.P.; et al. Removal of antibiotics, antibiotic-resistant bacteria and their associated genes by graphene-based TiO_2 composite photocatalysts under solar radiation in urban wastewaters. *Appl. Catal. B Environ.* **2018**, *224*, 810–824. [CrossRef]
107. Zhu, N.; Li, C.; Bu, L.; Tang, C.; Wang, S.; Duan, P.; Yao, L.; Tang, J.; Dionysiou, D.D.; Wu, Y. Bismuth impregnated biochar for efficient estrone degradation: The synergistic effect between biochar and Bi/Bi_2O_3 for a high photocatalytic performance. *J. Hazard. Mater.* **2020**, *384*, 121258. [CrossRef]
108. Song, W.; Zhao, J.; Xie, X.; Liu, W.; Liu, S.; Chang, H.; Wang, C. Novel BiOBr by compositing low-cost biochar for efficient ciprofloxacin removal: The synergy of adsorption and photocatalysis on the degradation kinetics and mechanism insight. *RSC Adv.* **2021**, *11*, 15369–15379. [CrossRef]
109. Thiruppathi, M.; Leeladevi, K.; Ramalingan, C.; Chen, K.C.; Nagarajan, E.R. Construction of novel biochar supported copper tungstate nanocomposites: A fruitful divergent catalyst for photocatalysis and electrocatalysis. *Mater. Sci. Semicond. Process.* **2020**, *106*, 104766. [CrossRef]